doi:10.1246/cl.2010.654

Published on the web May 19, 2010

Photostability of Water-dispersible CdTe Quantum Dots: Capping Ligands and Oxygen

Saim Emin,[1,3] Alexandre Loukanov,[2] Masanobu Wakasa,[1] Seiichiro Nakabayashi,*[1] and Yasuko Kaneko[4]
[1]*Department of Chemistry, Faculty of Science, Saitama University, Saitama 338-8570*
[2]*Laboratory of Engineering Nanobiotechnology, Department of Engineering Geoecology, University of Mining and Geology, Sofia 1700, Bulgaria*
[3]*National Institute for Materials Science (NIMS), Advanced Photovoltaics Center, 1-2-1 Sengen, Tsukuba 305-0047*
[4]*Faculty of Education, Saitama University, Saitama 338-8570*

(Received March 25, 2010; CL-100293; E-mail: sei@chem.saitama-u.ac.jp)

Here we report the effect of various capping ligands on the optical properties and photostability of CdTe quantum dots in aqueous solutions. Ligand exchange procedure is used to prepare water dispersive CdTe nanocrystals capped with aminoethanethiol, 3-mercaptopropionic and dihydrolipoic acids. The dynamics of photoexcited states is examined by transient photoluminescent spectroscopy. Our results demonstrate that the luminescence intensity of water-dispersible CdTe quantum dots is strongly influenced by molecular oxygen under light irradiation.

The research interest in inorganic semiconductor nanoparticles (also known as quantum dots, QDs) arises since they are successfully used in biology and medicine as intravascular probes for diagnostic (e.g., imaging) or therapeutics (e.g., drug delivery).[1,2] This great bioapplication of QDs is based on their unique properties of solubility in water, long fluorescence lifetimes, narrow emission spectra, and high quantum yield.[3] To reduce the release of toxic heavy atoms (Cd^{2+}) the QDs must be capped by a nontoxic ligand layer. This postsynthetic technique permits tailoring the solubility of fluorescent nanoparticles in aqueous buffers.[4] Functionalization of the quantum dots enables their application as luminescent probes in bioimaging.[5] Nevertheless, the newly formed capping ligands influence the optical properties and the photostability of QDs, especially when the particles are dispersed in water environment in the presence of oxygen and light irradiation.[6,7]

In this report we have investigated the influence of oxygen and light irradiation on the photostability of water-dispersible CdTe nanocrystals functionalized with various ligands. We have employed ligands that are widely used in QD functionalization such as aminoethanethiol (AET), 3-mercaptopropionic acid (MPA), and dihydrolipoic acid (DHLA).[4,7] To investigate the fluorescence quenching of QDs that is caused by molecular oxygen we applied cyclic voltammetry (CV) for "in situ" monitoring of molecular oxygen in QD solutions. To the best of our knowledge this is the first study that utilizes cyclic voltammetry for evaluation of oxygen in QD solutions. The result from CV allowed us to draw straightforward relation between oxygen concentration and emission quenching of QDs. We found that the photostability of QDs is strongly influenced by oxygen (O_2) concentration. In this work we investigated the effect of the capping ligands on the optical properties of QDs at fixed nanocrystal size. Moreover, the use of photostable and water-dispersible QDs is important for bioimaging and photovoltaic applications.

CdTe nanocrystals are synthesized in hot-matrix (see Supporting Information[8]), and their optical properties are characterized by absorption and photoluminescence (PL) spectroscopy as shown on Figure 1. From the excitonic absorption peak, the sizes of the nanocrystals are calculated.[9] The PL spectra of the nanocrystals display clear band-edge recombination without any trap-state-related emission.

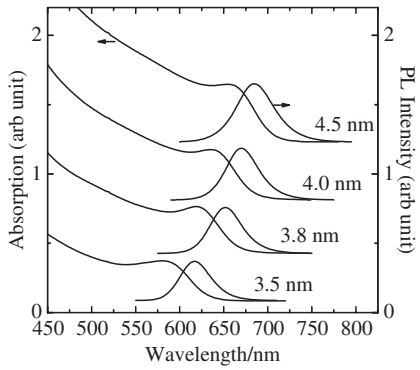

Figure 1. Absorption and photoluminescence spectra of CdTe QDs in choloroform ($\lambda_{ex} = 450$ nm).

The fluorescence decay curves of water-dispersible CdTe nanocrystals (in Ar atmosphere) are shown on Figure 2. The intensity decays are fitted to a multiexponential model:[10]

$$I(t) = \sum_{i=1}^{2} \alpha_i \exp(-t/\tau_i) \quad (1)$$

Where τ_i is the decay time and α_i is a pre-exponential factor. The decay times are determined from the global fit. The shape of the decay curves of CdTe–MPA QDs synthesized in this study differs from the results for CdTe–MPA QDs synthesized in dodecylamine.[11] Distribution of decay times causing nonexponential decays in QDs has been discussed in terms of variations in the nonradiative decay rates caused by surface trap states.[12,13] Furthermore, substitution of the average fluorescence lifetimes obtained from Figure 2 allows us to calculate the radiative (k_r) and nonradiative decay (k_{nr}) rates[14,15]

$$\Phi = \frac{k_r}{k_r + \sum k_{nr}} = k_r \tau \quad (2)$$

where Φ is the experimentally determined fluorescence quantum yield in inert gas atmosphere. The quantum yields and the radiative and nonradiative decay rates are shown in Table 1. Both fluorescence lifetimes and radiative decay rates of QDs decrease in the following order: MPA > AET > DHLA.

In spite of its role to preserve the quantum yield of fluorescence, the ligand MPA suffers from disadvantages such as

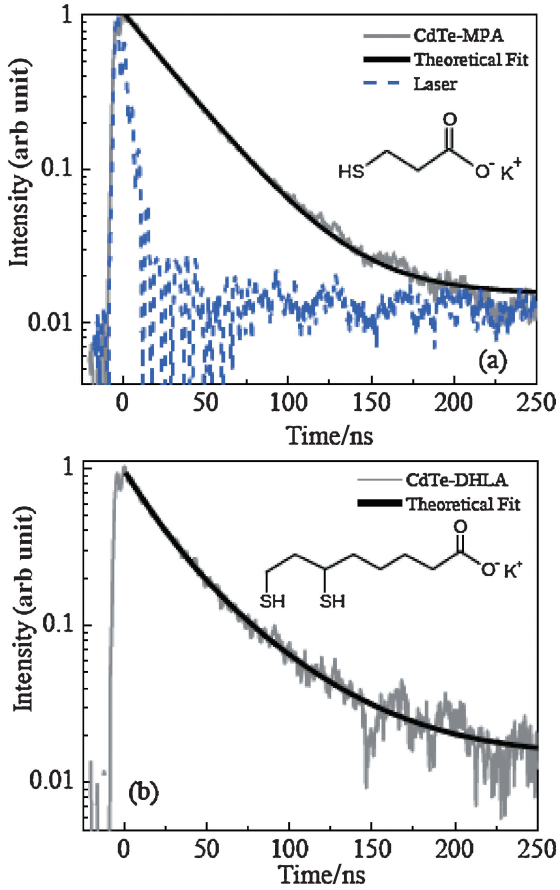

Figure 2. Decay curves of CdTe QDs ($d = 4.3$ nm) capped with (a) MPA and (b) DHLA ($\lambda_{ex} = 355$ nm).

Table 1. Quantum yields and fluorescence lifetimes of CdTe QDs ($d = 4.3$ nm) capped with various ligands

Ligand	Φ^a	α_1	τ_1 /ns	α_2	τ_2 /ns	τ_{av} /ns	$k_r \times 10^6$ /s^{-1}	$k_{nr} \times 10^7$ /s^{-1}
MPA	0.25	0.52	32.6	0.52	32.6	32.6	7.9	2.3
AET	0.13	0.95	27.8	0.03	176	32.3	4.3	2.7
DHLA	0.03	0.71	20.5	0.22	64.3	30.9	1.2	3.1

[a]Absolute fluorescence quantum yield.

having a short chain that reflects the photostability of the QDs upon irradiation with light (in O_2).

Photoluminescence quenching of MPA-capped CdTe QDs by oxygen is shown in Figure 3a. The PL quenching efficiency depends on the concentration of oxygen. A similar effect is observed for DHLA-capped CdTe QDs as well (Figure 3b). It seems that the longer DHLA ligand (ca. 1.2 nm) serves as a robust layer in protecting the QDs surface from water molecules. Contrary to DHLA, the MPA ligand is relatively short (ca. 0.7 nm) bringing to close proximity the QDs and the water molecules.[8] The latter favors photoinduced electron transfer from the QDs to oxygen molecule.[8] Final "destination" for the photoinduced electrons is expected to be the water molecule (eq 7).

The process of light absorption by CdTe nanocrystals creates an electron–hole pair:

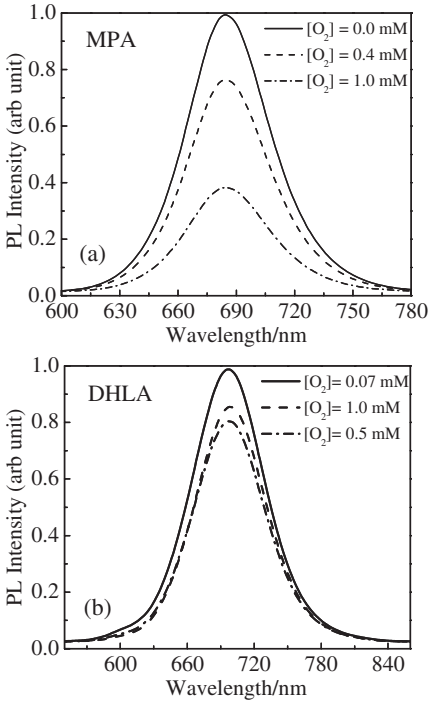

Figure 3. (a) PL spectra of 1.2×10^{-6} M CdTe–MPA and (b) 1.2×10^{-6} M CdTe–DHLA QDs exposed to varying levels of oxygen.

$$\mathrm{CdTe} + h\nu \rightarrow \mathrm{CdTe}(h^+ + e^-) \quad (3)$$

If an electron scavenger is absent from the system, the electron–hole pair is limited to recombination:

$$\mathrm{CdTe}(h^+ + e^-) \rightarrow \mathrm{CdTe} + h\nu \quad (4)$$

However, when there is a scavenger in the system such as molecular oxygen electron transfer to the scavenger occurs, leaving behind a hole in the CdTe lattice:

$$\mathrm{CdTe}(h^+ + e^-) + O_2 \rightarrow \mathrm{CdTe}(h^+) + O_2(e^-) \quad (5)$$

The excess holes remaining in the valence band of CdTe nanocrystal induce anodic corrosion similar to that reported earlier in CdSe colloids.[16,17] In fact, photodegradation of CdTe–MPA nanocrystals is observed upon continuous illumination with light (in O_2).[8]

The PL peaks from Figure 3 are plotted as a function of oxygen concentration as shown in the inset of Figure 4. The data are fitted with straight lines.[18] The slope of these lines, K_{SV}, provides a practical measure of quenching efficiency. The larger K_{SV}, the more efficient the quencher. From the plot it follows that the electrons are scavenged by oxygen better in the case of MPA ligand, $K_{SV} = 1.66$ (l/mmol) compared with DHLA ligand, $K_{SV} = 0.18$ (l/mmol). From these values we conclude that quenching occurs predominantly through static quenching pathways.[8] An identical effect of luminescence quenching in MPA- and DHLA-capped CdTe QDs is observed with methylviologen as well ($K_{SV} \approx 10^6$ M^{-1}).[8] Therefore, the observed large K_{SV} is due to the length of the capping ligand.

"In situ" detection of oxygen in QD solutions is achieved by cyclic voltammetry. The voltammograms are recorded on a

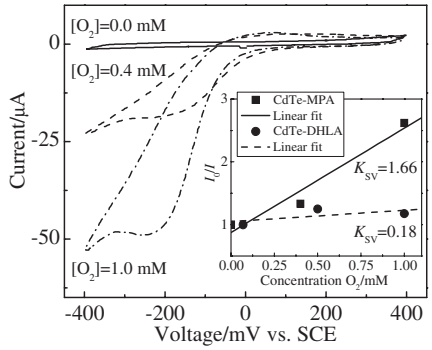

Figure 4. Cyclic voltammogram of dioxygen in 1.2×10^{-6} M CdTe–MPA QDs solution (4×10^{-1} M $NaClO_4$) at a platinum electrode, $\nu = 80\,\mathrm{mV\,s^{-1}}$. The inset is a Stern–Vomer plot that gives relation between fluorescence intensity versus oxygen concentration.

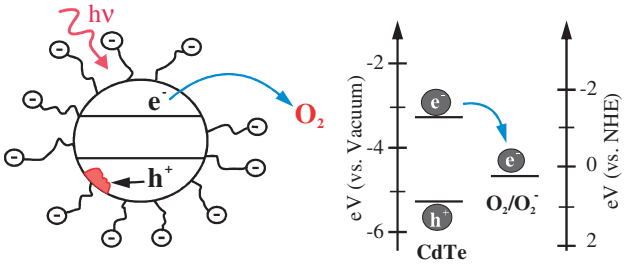

Scheme 1. Photoinduced electron-transfer scheme from CdTe to oxygen and representative energy levels.

platinum electrode with a well-defined surface area, A.[8] By substituting the value of A in the Randles–Sevcik equation, the concentration of oxygen is calculated:[19]

$$i_p = (2.65 \times 10^5) n^{3/2} A D^{1/2} C \nu^{1/2} \quad (6)$$

where i_p is the cathodic current associated with the chemical reaction, n is the number of electrons ($n = 2$), D is the diffusion constant, D (O_2) $= 1.97 \times 10^{-5}$ ($\mathrm{cm^2\,s^{-1}}$), C is the concentration ($\mathrm{mol\,cm^{-3}}$), and ν is the sweep rate ($\mathrm{V\,s^{-1}}$).

Cyclic voltammograms of oxygen in CdTe–MPA QD solutions (1.2×10^{-6} M) in the presence of $NaClO_4$ supporting electrolyte (4×10^{-1} M) are shown in Figure 4. The appearance of a peak at ca. -200 mV indicates the reduction potential of oxygen at the platinum electrode. The process of dioxygen reduction is totally irreversible with two-electron stoichiometry:[20]

$$O_2 + 2H_3O^+ + 2e^- \rightarrow HOOH + 2H_2O \quad (7)$$

Equation 7 is useful to reveal the mechanism of electron transport in QD solution. Moreover, photoinduced electron transfer from QDs[21] to oxygen is energetically favored as shown in Scheme 1.

Furthermore, irradiation (in O_2) of QDs with light for short times causes mainly surface changes. However, irradiation for longer times induces degradation of the QDs.[8] In conclusion, the photostability of CdTe QDs in aqueous environment is strongly dependent on the length of the ligands used to cover the nanocrystals. Nanoparticles covered with MPA ligands possesses high quantum yield but low photostability. In contrast to MPA, the QDs functionalized with DHLA exhibit low quantum yield but high photostability. Therefore, compromise is needed between the quantum yield and photostability of QDs for the specific application.

S. Emin is thankful to the Ministry of Education, Culture, Sports, Science and Technology of Japan (Monbusho) for the granted Ph.D. scholarship. The authors thank Prof. Yasuhiro Uozumi (Institute for Molecular Science, Okazaki) for his kind permission to use the field emission electron microscope.

References and Notes

1 C. M. Niemeyer, *Angew. Chem., Int. Ed.* **2001**, *40*, 4128.
2 A. Loukanov, N. Kamasawa, R. Danev, R. Shigemoto, K. Nagayama, *Ultramicroscopy* **2010**, *110*, 366.
3 X. Michalet, F. F. Pinaud, L. A. Bentolila, J. M. Tsay, S. Doose, J. J. Li, G. Sundaresan, A. M. Wu, S. S. Gambhir, S. Weiss, *Science* **2005**, *307*, 538.
4 A. R. Clapp, I. L. Medintz, H. T. Uyeda, B. R. Fisher, E. R. Goldman, M. G. Bawendi, H. Mattoussi, *J. Am. Chem. Soc.* **2005**, *127*, 18212.
5 F. Chen, D. Gerion, *Nano Lett.* **2004**, *4*, 1827.
6 J. Ma, J.-Y. Chen, J. Guo, C. C. Wang, W. L. Yang, L. Xu, P. N. Wang, *Nanotechnology* **2006**, *17*, 2083.
7 J. Ma, J.-Y. Chen, Y. Zhang, P.-N. Wang, J. Guo, W.-L. Yang, C.-C. Wang, *J. Phys. Chem. B* **2007**, *111*, 12012.
8 Supporting Information is available electronically on the CSJ-Journal Web site, http://www.csj.jp/journals/chem-lett/index.html.
9 W. W. Yu, L. Qu, W. Guo, X. Peng, *Chem. Mater.* **2003**, *15*, 2854.
10 J. R. Lakowicz, *Principles of Fluorescence Spectroscopy*, Springer, New York, **2006**.
11 S. Wuister, I. Swart, F. V. Driel, S. Hickey, C. D. M. Donegá, *Nano Lett.* **2003**, *3*, 503.
12 A. Rogach, T. Franzl, T. Klar, J. Feldmann, N. Gaponik, V. Lesnyak, A. Shavel, A. Eychmüller, Y. Rakovich, J. Donegan, *J. Phys. Chem. C* **2007**, *111*, 14628.
13 G. Morello, M. Anni, P. D. Cozzoli, L. Manna, R. Cingolani, M. De Giorgi, *J. Phys. Chem. C* **2007**, *111*, 10541.
14 The amplitude weighted average fluorescence lifetimes were calculated from the relation: $\tau_{av} = (\alpha_1\tau_1 + \alpha_2\tau_2)/(\alpha_1 + \alpha_2)$.
15 J. M. D. Rodríguez, J. A. H. Melián, J. P. Peña, *J. Chem. Educ.* **2000**, *77*, 1195.
16 K. Tvrdy, P. V. Kamat, *J. Phys. Chem. A* **2009**, *113*, 3765.
17 N. M. Dimitrijevic, P. V. Kamat, *J. Phys. Chem.* **1987**, *91*, 2096.
18 The plot in Figure 4 is a Stern–Volmer plot, $I_0/I = 1 + K_{SV}[O_2]$, where I_0 is the QDs luminescence intensity without a quencher, I is the QDs luminescence intensity in the presence of a quencher, K_{SV} is the Stern–Volmer quenching constant, and [O_2] is the concentration of oxygen. The constant $K_{SV} = k_q\tau$, where k_q is the static quenching constant and τ is the fluorescence lifetime without quencher species. The static quenching constant is calculated from the average fluorescence lifetime, τ_{av}, $k_q = 5.1 \times 10^{10}\,\mathrm{M^{-1}\,s^{-1}}$ (MPA) and $k_q = 5.8 \times 10^9\,\mathrm{M^{-1}\,s^{-1}}$ (DHLA).
19 A. J. Bard, L. R. Faulkner, *Electrochemical Methods: Fundamentals and Applications*, John Wiley&Sons, New York, **2000**.
20 D. T. Sawyer, A. Sobkowiak, J. L. Roberts, *Electrochemistry for Chemists*, John Wiley & Sons, New York **1995**, p. 369.
21 S.-C. Cui, T. Tachikawa, M. Fujitsuka, T. Majima, *J. Phys. Chem. C* **2008**, *112*, 19625.

